Temperature Dependence of Unbinding Forces between Complementary DNA Strands

Irina Schumakovitch, Wilfried Grange, Torsten Strunz, Patricia Bertoncini, Hans-Joachim Güntherodt, and Martin Hegner

Department of Physics and Astronomy, National Center of Competence in Research (NCCR) on Nanoscale Science, University of Basel, CH-4056 Basel, Switzerland

ABSTRACT   Force probe techniques such as atomic force microscopy can directly measure the force required to rupture single biological ligand receptor bonds. Such forces are related to the energy landscape of these weak, noncovalent biological interactions. We report unbinding force measurements between complementary strands of DNA as a function of temperature. Our measurements emphasize the entropic contributions to the energy landscape of the bond.

INTRODUCTION

Unbinding forces of weak, noncovalent bonds have been measured by atomic force microscopy (AFM) (Florin et al., 1994; Lee et al., 1994; Moy et al., 1994; Dammer et al., 1995; Hinterdorfer et al., 1996; Allen et al., 1997) or biomembrane force probes (Evans, 1998). In addition to being of direct interest for cell adhesion (Bongrand, 1999; Zhu, 2000), studies can give a unique insight into the geometry of the energy landscape of such a bond.

To understand the relation between force and energy landscape, one can consider an AFM experiment in which the spring used to measure the forces acting on the molecular complex is weak compared with the molecular bond stiffness. The ligand is immobilized on a sharp tip attached to a microfabricated cantilever and the receptor is immobilized on a surface. When approaching the surface to the tip, a specific bond may form between ligand and receptor, e.g., complementary DNA strands. The bond is then loaded with an increasing force when retracting the surface from the tip (dynamic force spectroscopy (DFS)). At a certain force, ligand and receptor unbind, giving rise to an abrupt jump of the tip away from the surface (Fig. 1). Evans and Ritchie (1997) demonstrated that the unbinding is caused by thermal fluctuations rather than by a mechanical instability. If the thermal lifetime of the bond is short compared with the time it takes to build up an observable force during a slow loading process, no unbinding event is observed. With faster loading, finite unbinding forces are observed. Therefore, unbinding forces depend on the rate of loading and on the details of the functional relationship between bond lifetime and an applied force.

One challenge in DFS measurements is to investigate parameters that are not accessible by conventional bulk methods. In particular, a complete characterization of the energy landscape of the bond (location, height, and bond lifetime of the different energy barriers along the reaction coordinate) can be directly obtained from a plot of the most probable unbinding force as a function of the loading rate (Evans, 2001). So far, ligand-receptor bonds having a low degree of conformational fluctuations have been extensively studied and well characterized (Merkel, 2001). Also, theory was able to reproduce the experimental trends observed in the above mentioned complexes, such as the biotin-
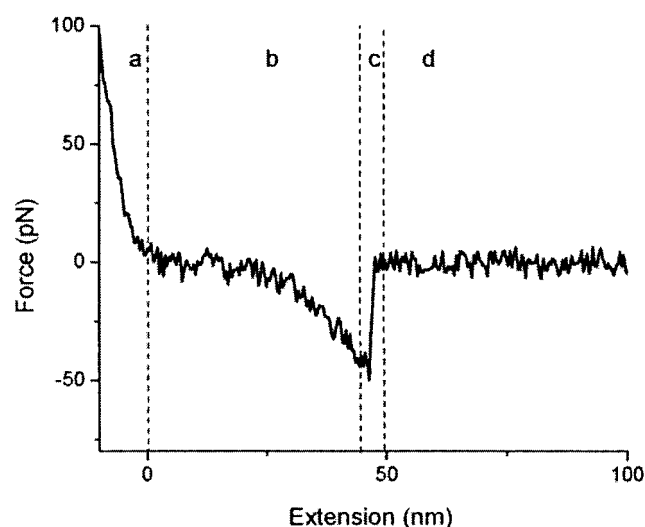

FIGURE 1   A typical force-distance curve obtained in a stretching AFM experiment (retraction cycle). A DNA strand (TATTAATATCAAGTTG) is immobilized by its 5′-end via a PEG linker on the AFM tip and its complement is attached in a similar fashion by its 5′-end to the surface. When the tip is approached close to the surface a specific bond between the two strands is formed (a). The AFM tip is then retracted from the surface at constant loading rate ((b) [PEG stretching]). The sudden drop in the force curve reflects unbinding of the duplex ((c) [specific DNA unbinding]). The loading rate r (retract velocity v times the elasticity c) is determined from the slope of the force-displacement curve before the unbinding event occurs.

(strept)avidin bond (Merkel et al., 1999; Galligan et al., 2001). The situation might be less straightforward for systems undergoing a large degree of conformation changes upon unbinding, such as DNA. First, many reaction paths exist in the energy landscape that are separated by less than thermal energy. Second, the shape of the energy landscape should be greatly modified when the temperature is changed. In this case, temperature-dependent DFS measurements should be evidence for different reaction pathways, in contrast to what could be observed for rigid bonds.

In this work, we investigate the unbinding of complementary strands of ssDNA that are pulled apart at their opposite 5′-ends. We choose the DNA sequence 5′-TATTAATAT-CAAGTTG with its complement where the thermodynamic data, especially the lifetime of the duplex as a function of temperature, have been determined (Tibanyenda et al., 1984).

MATERIALS AND METHODS

Surface and tip modification

All chemicals were purchased from Fluka Chemical Corporation (Milwaukee, WI) unless noted otherwise. Glass slides were cleaned in ethanol for 20 min in an ultrasonic bath and were dried under a stream of argon. From now on, both surfaces, the glass slides, and the AFM-tips (Si$_3$Ni$_4$-Microlever, Park Scientific, Sunnyvale, CA), were treated in parallel. The surfaces were silanized immediately after a 60 min treatment with a strong ultraviolet (UV) light source (UV-Clean, Boekel Scientific, Feasterville, PA) in a 2% solution of aminopropyltriethoxysilane in dry toluene for 2 h. After rinsing with toluene and drying under a stream of argon, the surfaces were immersed in a 1 mM solution of poly(ethylene glycol)-α-maleimide-ω-N-hydroxy-succinimide-ester (molecular weight 3400; Shearwater Polymers, Huntsville, AL) in DMSO for 2–3 h. The surfaces again were rinsed with DMSO and were dried in a stream of argon.

The oligonucleotides with a 5′-SH modification were synthesized by Microsynth (Balgach, Switzerland) and were stored in a pH 6.5 phosphate buffer containing 10 mM dithiothreitol at 21°C until use. Immediately before use, the oligonucleotides were diluted to a final concentration of 25 mM with a pH 6.5 phosphate buffer, and dithiothreitol was extracted from an aliquot of typically 200 ml by washing three times with 1 ml of ethylacetate. A 50-ml drop of the oligonucleotide solution was then incubated on the poly(ethylene glycol)-α-maleimide-modified surfaces overnight at room temperature in a humid chamber. After rinsing with PBS buffer (pH 7.3; Life Technologies, Rockville, MD), the tips and surfaces were ready for use in the force experiments.

DFS measurements

DFS measurements were performed using a commercial AFM instrument (Nanoscope III, Digital Instruments, Santa Barbara, CA). AFM cantilevers used for this experiment had spring constants <20 pN/nm. Each cantilever was in situ calibrated according to the method of Hutter (Hutter and Bechhoefer, 1993). The temperature was controlled using a homebuilt fluid cell where the buffer solution (25 mM sodium phosphate, 1 mM sodium cacodylate, 0.1 mM EDTA, pH 7.0, 0.2 M NaCl (Tibanyenda et al., 1984)) that immersed both the probe surface and the AFM cantilever was in contact with a Peltier element (Melcor, Trenton, NJ), driven with a constant current source. The temperature of the buffer was monitored with a thermocouple (Thermocoax, Suresnes, France). The thermocouple was calibrated with a digital thermometer and temperature measurements at different points of the cell showed deviations <2°C.

LOADING RATE DEPENDENCE OF THE APPLIED FORCE

For all ligand receptor systems investigated so far, a linear increase of the unbinding forces with the logarithm of the loading rate has been observed (Merkel, 2001). Similar behavior has been shown for the unfolding of proteins, at least in the limit of small forces. This is a direct consequence of an exponential decrease of the bond lifetime with an applied force (Evans, 2001). Bell (1978) first postulated that an applied force F decreases the energy for dissociation ΔE_0 linearly, i.e.,:

$$\Delta E = \Delta E_0 - xF, \tag{1}$$

and that the bond lifetime $\tau(F)$ is given by an Arrhenius expression:

$$\tau(F) = \tau_0 e^{\Delta E/k_B T}, \tag{2}$$

where τ_0 is a frequency prefactor and $k_B T$ the thermal energy.

The bond length x describes the geometry of the energy landscape. It is interpreted as the distance between the ground state and an energy barrier along the dissociation path (the reaction coordinate), projected onto the direction of the applied force. Note that in principle many reaction pathways exist, but the applied force is expected to select a specific reaction coordinate in the multidimensional energy landscape. In other words, the system will follow the reaction pathway corresponding to the lowest energy barriers. From Eqs. 1 and 2, we can easily estimate the thermal off-rate $K_{off}(F)$ of a bond under an applied force:

$$k_{off}(F) = K_{off}\exp(F/F^0), \tag{3}$$

where K_{off} is the natural thermal off-rate for dissociation and F^0 is a force-scale factor ($F^0 = k_B T/x$). Although the bond lifetime is a relevant parameter to describe the kinetics of bond rupture, the quantity directly measured in a typical AFM experiment is an unbinding force. However, because the rupture of a bond is a stochastic process, we can not expect to measure only one specific unbinding force. Rather, the measured unbinding force should follow a distribution whose width is mainly determined by the force-scale factor. In this case, it can be shown that the most probable unbinding force should depend on the applied loading rate r as (Evans, 1998):

$$F* = F^0\ln\left(\frac{r}{F^0 K_{off}}\right), \tag{4}$$

Because each linear regime found in an $F*(\ln(r))$ plot corresponds to a specific energy barrier, a map of the energy landscape can be determined using DFS experiments. One should state, however, that only a portion of the energy landscape is probed for typical DFS experiments because of the limited range of loading rate accessible (Galligan et al., 2001). Let us finally mention that Eq. 4 is valid in the limit of rigidly connected bond. When weak bonds are connected by polymer chains such as PEG linkers for instance, the $F*(\ln(r))$ plot is nonlinear at low forces (Evans and Ritchie, 1999). However, we checked that correcting Eq. 4 for the elasticity of poly(ethylene)glycol (PEG) linkers only slightly changes the absolute of the length x (included in the statistical errors presented in Figs. 4 and 5) without affecting the trends observed in the temperature dependence of x (see below).

RESULTS

Probability distribution and specificity of the unbinding force

As mentioned above, unbinding events are caused by thermal fluctuations rather than by mechanical instability. Therefore unbinding forces show a distribution whose width σ is mainly determined by the force scale F^0, i.e., $\sigma = F^0(x)$.
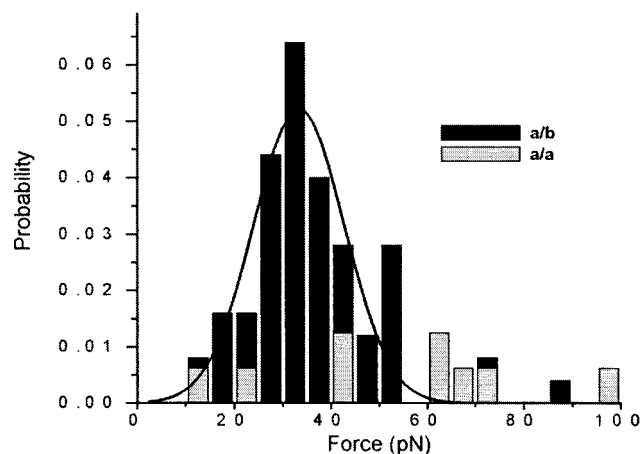
FIGURE 2 The probability distribution for the rupture force ($\sim$500 approach/retract cycles, retract velocity 400 nm/s). For this experiment, the TATTAATATCAAGTTG oligomer *a* was attached to the tip of the AFM-cantilever and its complement *b* was immobilized on the surface (complements were pulled apart in their 5'-5' directions). Black rectangles (*a* against *b*), gray rectangles (*a* against *a*), solid line: Gaussian fit. The force distribution shows that the measured unbinding force results from a specific *a* against *b* interaction.

When approaching the tip to the surface, some nonspecific attachments may occur, even in the presence of treated surfaces or pure polymer samples. Therefore, it is imperative to test the specificity of the interaction (Fig. 2). Unspecific interactions can be minimized using linkers (e.g., PEG linkers) that shift the region where unbinding takes place away from the surface.

Finally, to quantify the most probable value for the unbinding force of a single complex, one has to work under conditions in which the probability that two or more duplexes are attached to the tip is low. These conditions are fulfilled for a low concentration and when the linkers have a length that is comparable with the diameter of the AFM-tip ($\sim$40 nm). In this case, it is very unlikely that two or more linkers are extended to the same length when stretched. However, subsequent rupture events may be found. But still, the last rupture event will occur for an applied force equal to F^*.

Temperature-dependent rupture force of a single bond

Fig. 3 shows that the scaling of the most probable unbinding force is logarithmic in the loading rate for loading rates from 60 to 10 000 pN/s and temperatures 11° and 36°C. This allows a fit of the data and determines the lifetime at zero force τ_{off} and the length x. The change of τ_{off} ($1/K_{off}$) with temperature is clearly indicated by the change in the loading rate where the force vanishes. The visible change of the slope with temperature indicates a temperature dependence of the length x (Eq. 4).
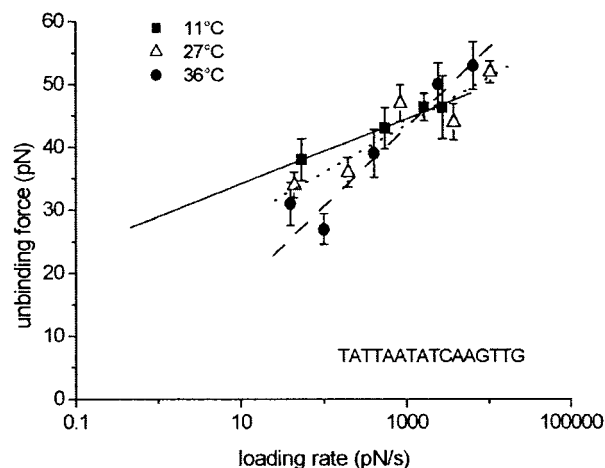

FIGURE 3 Velocity dependence of the most probable unbinding force as a function of temperature. Squares (T = 11°C), triangles (27°C), circles (36°C). From this plot, both the length x and the natural thermal off-rate can be determined (Eq. 4). Each datapoint comprises a set of $\sim$500 approach/retract cycles. Lines correspond to a linear fit according to Eq. 4. Solid line (T = 11°C), dots (27°C), dashed line (36°C).

Comparison with bulk experiments

The thermal lifetime extracted from the unbinding force measurements in the temperature range from 6° to 36°C can now be compared with lifetime measurements with the temperature jump (TJ) method near the melting transition (35° to 50°C) of the duplex (Fig. 4). From the slope of the $\log(\tau_{off})$ versus $1/T$ plot, we find the activation enthalpy for dissociation $\Delta H_{AFM} = 300 \pm 42$ kJ/mol compared with $\Delta H_{TJ} = 375 \pm 16$ kJ/mol (Tibanyenda et al., 1984). The good agreement of the bond lifetime from force measurements with the TJ values ensures that the Bell ansatz cor-
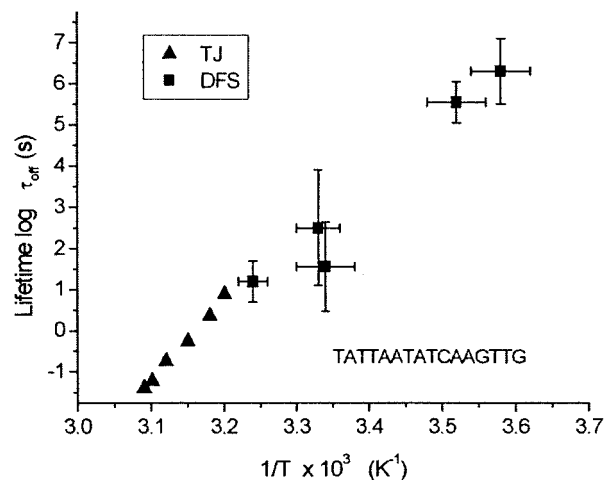

FIGURE 4 Lifetimes from the fit of the data of Fig. 3 with Eq. 4 in function of the inverse temperature ($1/T$). DFS experiments (*squares*), TJ experiments (Tibanyenda et al., 1984) (*triangles*).
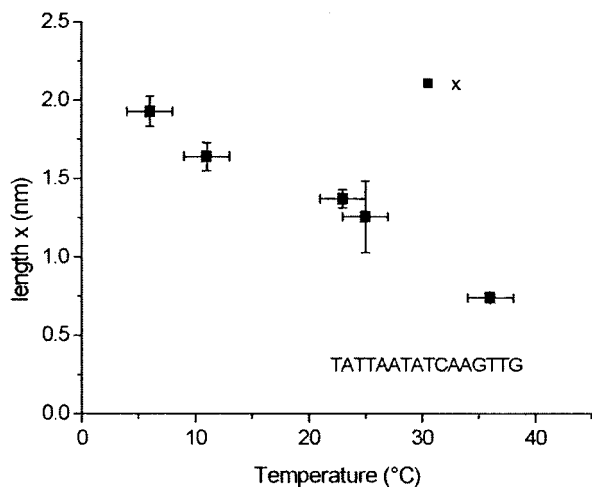
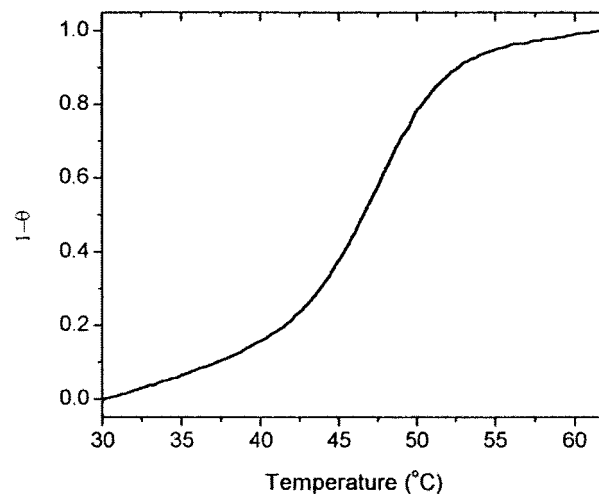FIGURE 5 Bond length x as a function of the temperature.

FIGURE 6 The melting curve (expressed in terms of the fraction of melted basepairs $1-\theta(T)$) obtained by measuring the change in the 260 nm UV absorption spectra as a function of temperature ($T_M \sim 48°C$). The buffer was identical to the one used for the AFM measurements [0.2 M NaCl] (Tibanyenda et al., 1984). Note that there is a 65% variation in the measured x values from 6° to 36°C, whereas the melting curve does not show any significant variation for this temperature range.

rectly describes the dissociation kinetics under an applied force for the DNA duplex. The small discrepancies may be attributed to surface effects. The length x, determined from our data, is thus well defined for all investigated temperatures (Fig. 5). Moreover, the good agreement between our data and the TJ measurements clearly indicates that we pull sufficiently slow to probe the last energy barrier for all temperatures investigated (Schwesinger et al., 2000).

DISCUSSION

As outlined previously, the temperature dependence of x is an intrinsic property of the system we study. Let us emphasize that the temperature dependence of x is not expected if one thinks in terms of a one-dimensional energy landscape with a sharp barrier for dissociation that leads to Eq. 2 (Bell, 1978; Hänggi et al., 1990). In the next section, we discuss possible explanations for the observed behavior of x.

Melting curve and basepair dependence

One way to interpret our results would be to state that the unbinding of DNA is a cooperative process so that the decrease of x with the temperature reflects the decreasing number of binding sites when the temperature approaches the melting temperature T_M.

In a previous paper, we have shown that the length x increases linearly with the number of binding sites (Strunz et al., 1999). This behavior is characteristic of bonds in series where each bond in the duplex contributes an increment in length along the direction of the applied force (Evans, 2001). Moreover, the average fraction of hydrogen-bonded basepairs $\theta(T)$ is temperature dependent. $\theta(T)$ can be factorized as: $\theta_{int}(T)\theta_{ext}(T)$, where $\theta_{int}(T)$ denotes the average fraction of bonded basepairs among the DNA duplex with at least one basepair, and $\theta_{ext}(T)$ is the fraction of DNA

strands which have at least one intact binding site with a complementary strand (Wartell and Benight, 1985). In the light of this result, we now realize that the decrease of x with the temperature could be associated to a corresponding decrease of $\theta_{int}(T)$. To verify this assumption, we measured the helix to coil transition curve of our DNA duplex using a temperature controlled UV absorption spectrometer. As shown in Fig. 6, $1-\theta(T)$ is almost constant for the range of temperatures investigated in our AFM experiment and can not explain the temperature dependence of x.

Variation of x with bond angle

We have previously mentioned that the length x denotes the distance from the ground state to the transition state. We also have outlined that the applied force selects this microscopic reaction coordinate. When an angle θ_F is introduced between the reaction coordinate and the applied force, the average length determined from DFS measurements is $\langle x \cdot \cos(\theta_F) \rangle$ (Evans, 1998). Assuming that the temperature would change θ_F, we could expect a variation in x. However, such an assumption has to be ruled out, as the use of PEG linkers (which are fully stretched for forces larger than a few pN) ensures that we always pull along the DNA-5′-5′ directions.

Multidimensional free energy landscape of a single bond

The decrease of x with the temperature can not be explained in terms of the melting properties of DNA neither in terms

of a change of external parameters (pulling direction). At this point, we would like to recall that many reaction paths, separated by energy barriers of comparable magnitude (close to $k_B T$), should exist for DNA, RNA, and proteins; i.e., systems that undergo a large degree of conformational changes upon unbinding. For these latter systems, the shape of the energy landscape changes with the temperature because of the competition between entropic and enthalpic contributions (Zhang and Chen, 2001). Therefore, measurements that directly probe the energy landscape should lead to different results (e.g., different x values) when the temperature is varied. And this is what is observed in our temperature-dependent DFS measurements.

Let us finally mention that for these latter systems, a gradual increase of the force should a priori lead to a change in the frequency occurrence of the different possible pathways. In this case, we can expect that Eq. 4 does not hold anymore (Merkel, 2001). However, the linear regime observed in the different $F^*(\ln(r))$ plot and the good agreement found between DFS and TJ measurements show that Eq. 4 should still be a good approximation to describe the dissociation of the duplex.

CONCLUSION

Using DFS measurements we have investigated the temperature dependence of the unbinding forces between complementary DNA strands attached at their $5'$-ends. In agreement with previous studies on this system (Strunz et al., 1999; Pope et al., 2001), the most probable unbinding force was found to depend on the loading rate. From this dependence, both the natural thermal off-rate for dissociation K_{off} and the bond length x along the reaction coordinate were determined. Our measured K_{off} values are in agreement with bulk temperature measurements, indicating the validity of our measurements. Interestingly, the length x shows a strong temperature dependence. This behavior, which is not expected in the case of one-dimensional energy landscape with a sharp energy barrier, indicates the role played by entropic contributions when unbinding DNA and unfolding RNA or proteins. However, the linear decrease of x with the temperature is still an open question. It is obvious that the exact relationship between the bond length and the temperature is not straightforward, and calculations are needed to explain the observed properties.

REFERENCES

Allen, S., X. Y. Chen, J. Davies, M. C. Davies, A. C. Dawkes, J. C. Edwards, C. J. Roberts, J. Sefton, S. J. Tendler, and P. M. Williams. 1997. Detection of antigen-antibody binding events with the atomic force microscope. *Biochemistry.* 36:7457–7463.

Bell, G. I. 1978. Models for the specific adhesion of cells to cells. *Science.* 200:618–627.

Bongrand, P. 1999. Ligand-receptor interactions. *Rep. Prog. Phys.* 62: 912–968.

Dammer, U., O. Popescu, P. Wagner, D. Anselmetti, H. J. Güntherodt, and G. N. Misevic. 1995. Binding strength between cell-adhesion proteoglycans measured by atomic-force microscopy. *Science.* 267:1173–1175.

Evans, E., and K. Ritchie. 1997. Dynamic strength of molecular adhesion bonds. *Biophys. J.* 72:1541–1555.

Evans, E. 1998. Energy landscapes of biomolecular adhesion and receptor anchoring at interfaces explored with dynamic force spectroscopy. *Faraday Discuss.* 111:1–16.

Evans, E., and K. Ritchie. 1999. Strength of a weak bond connected flexible polymer chains. *Biophys. J.* 76:2439–2447.

Evans, E. 2001. Probing the relation between force–lifetime–and chemistry in single molecular bonds. *Annu. Rev. Biophys. Biomol. Struct.* 30: 105–128.

Florin, E. L., V. T. Moy, and H. E. Gaub. 1994. Adhesion forces between individual ligand-receptor pairs. *Science.* 264:415–417.

Galligan, E., C. J. Roberts, M. C. Davies, S. J. Tendler, and P. M. Williams. 2001. Simulating the dynamic strength of molecular interactions. *J. Chem. Phys.* 114:3208–3214.

Hänggi, P., P. Talkner, and M. Borkovec. 1990. Reaction-rate theory: 50 years after Kramers. *Rev. Mod. Phys.* 62:251–341.

Hinterdorfer, P., W. Baumgartner, H. J. Gruber, K. Schilcher, and H. Schindler. 1996. Detection and localization of individual antibody-antigen recognition events by atomic force microscopy. *Proc. Natl. Acad. Sci. U.S.A.* 93:3477–3481.

Hutter, J. L., and J. Bechhoefer. 1993. Calibration of atomic-force microscope tips. *Rev. Sci. Instrum.* 64:3342–3342.

Lee, G. U., L. A. Chrisey, and R. J. Colton. 1994. Direct measurement of the forces between complementary strands of DNA. *Science.* 266: 771–773.

Merkel, R., P. Nassoy, A. Leung, K. Ritchie, and E. Evans. 1999. Energy landscape of receptor-ligand bonds explored with dynamic force spectroscopy. *Nature.* 397:50–53.

Merkel, R. 2001. Force spectroscopy on single passive biomolecules and single biomolecular bonds. *Phys. Rep.* 346:343–385.

Moy, V. T., E. L. Florin, and H. E. Gaub. 1994. Intermolecular forces and energies between ligands and receptors. *Science.* 266:257–259.

Pope, L. H., M. C. Davies, C. A. Laughton, C. J. Roberts, S. J. Tendler, and P. M. Williams. 2001. Force-induced melting of a short DNA double helix. *Eur. Biophys. J.* 30:53–62.

Schwesinger, F., R. Ros, T. Strunz, D. Anselmetti, H. J. Güntherodt, A. Honegger, L. Jermutus, L. Tiefenauer, and A. Plückthun. 2000. Unbinding forces of single antibody-antigen complexes correlate with their thermal dissociation rates. *Proc. Natl. Acad. Sci. U.S.A.* 97:9972–9977.

Strunz, T., K. Oroszlan, R. Schäfer, and H. J. Güntherodt. 1999. Dynamic force spectroscopy of single DNA molecules. *Proc. Natl. Acad. Sci. U.S.A.* 96:11277–11282.

Tibanyenda, N., S. H. Debruin, C. A. Haasnoot, G. A. Vandermarel, J. H. Vanboom, and C. W. Hilbers. 1984. The effect of single base-pair mismatches on the duplex stability of d(t-a-t-t-a-a-t-a-t-c-a-a-g-t-t-g) · d(c-a-a-c-t-t-g-a-t-a-t-t-a-a-t-a). *Eur. J. Biochem.* 139:19–27.

Wartell, R. M., and A. S. Benight. 1985. Thermal denaturation of DNA molecules: a comparison of theory with experiment. *Phys. Rep.* 126: 67–107.

Zhang, W., and S. J. Chen. 2001. Predicting free energy landscapes for complexes of double-stranded chain molecules. *J. Chem. Phys.* 114: 4253–4266.

Zhu, C. 2000. Kinetics and mechanics of cell adhesion. *J. Biomech.* 33:23–33.